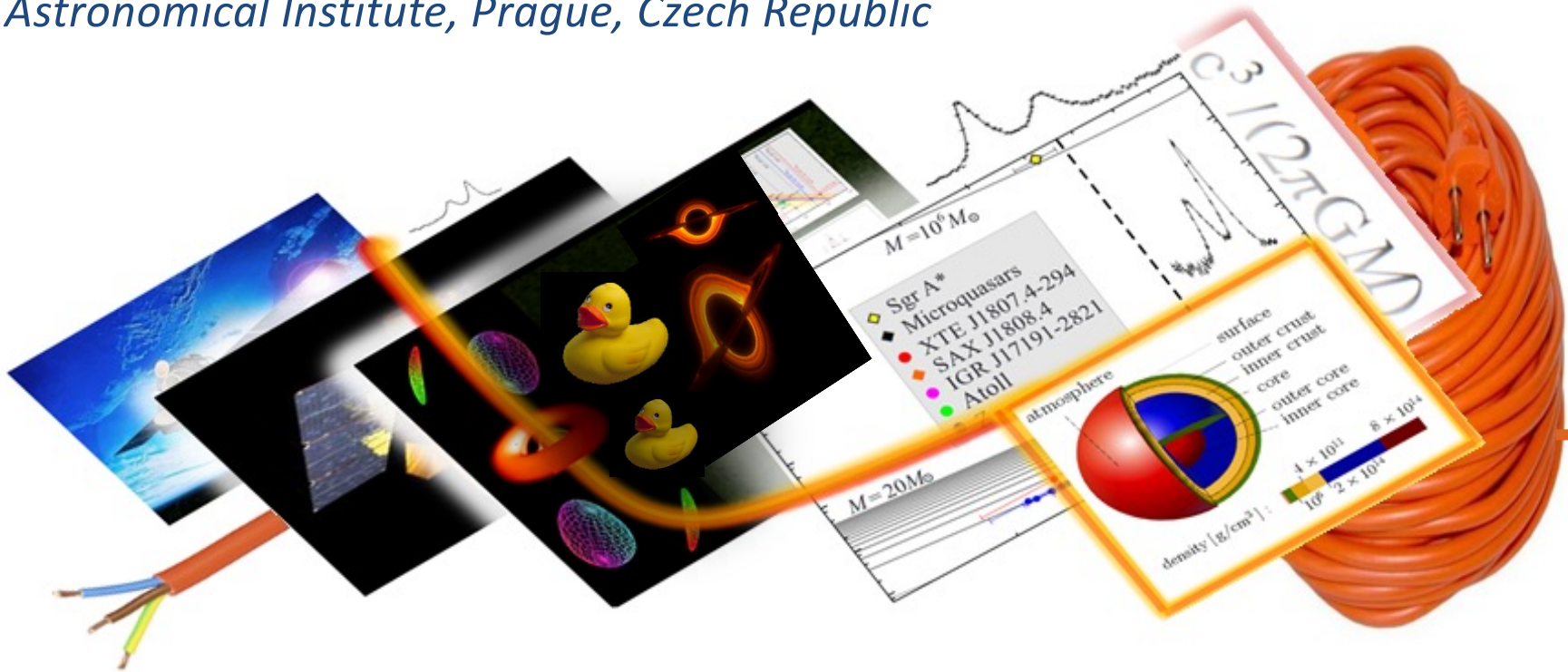


The mass, spin and rapid X-ray variability of accreting compact objects

** *Institute of Physics, Research Centre for Computational Physics and Data Analysis, Silesian University in Opava, Czech Republic*

* *Astronomical Institute, Prague, Czech Republic*



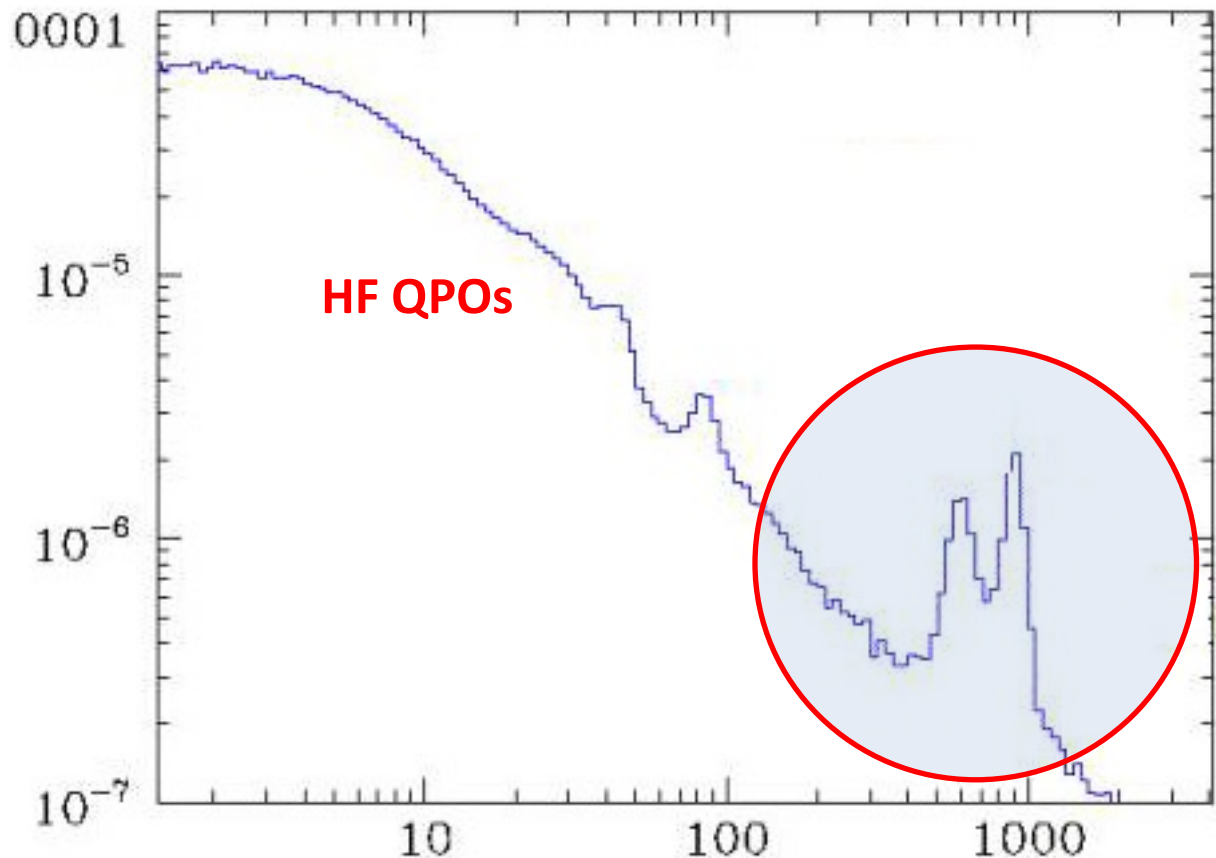
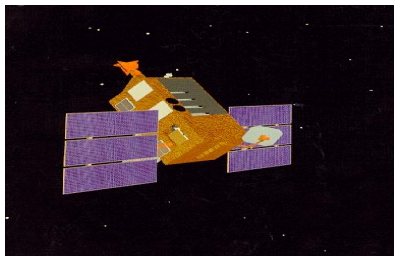
The mass, spin and rapid X-ray variability of accreting compact objects

Talk based mostly on

- *Török, Kotrlová, Matuszková, Klimovičová, Lančová, Urbancová, Šrámková (ApJ, 2022)*
- *Matuszková, Török, Klimovičová, Horák, Šrámková, Straub, Urbancová, Lančová, Urbanec, Karas (in prep.)*

1. Rapid variability of accreting compact objects, HF QPOs and GR

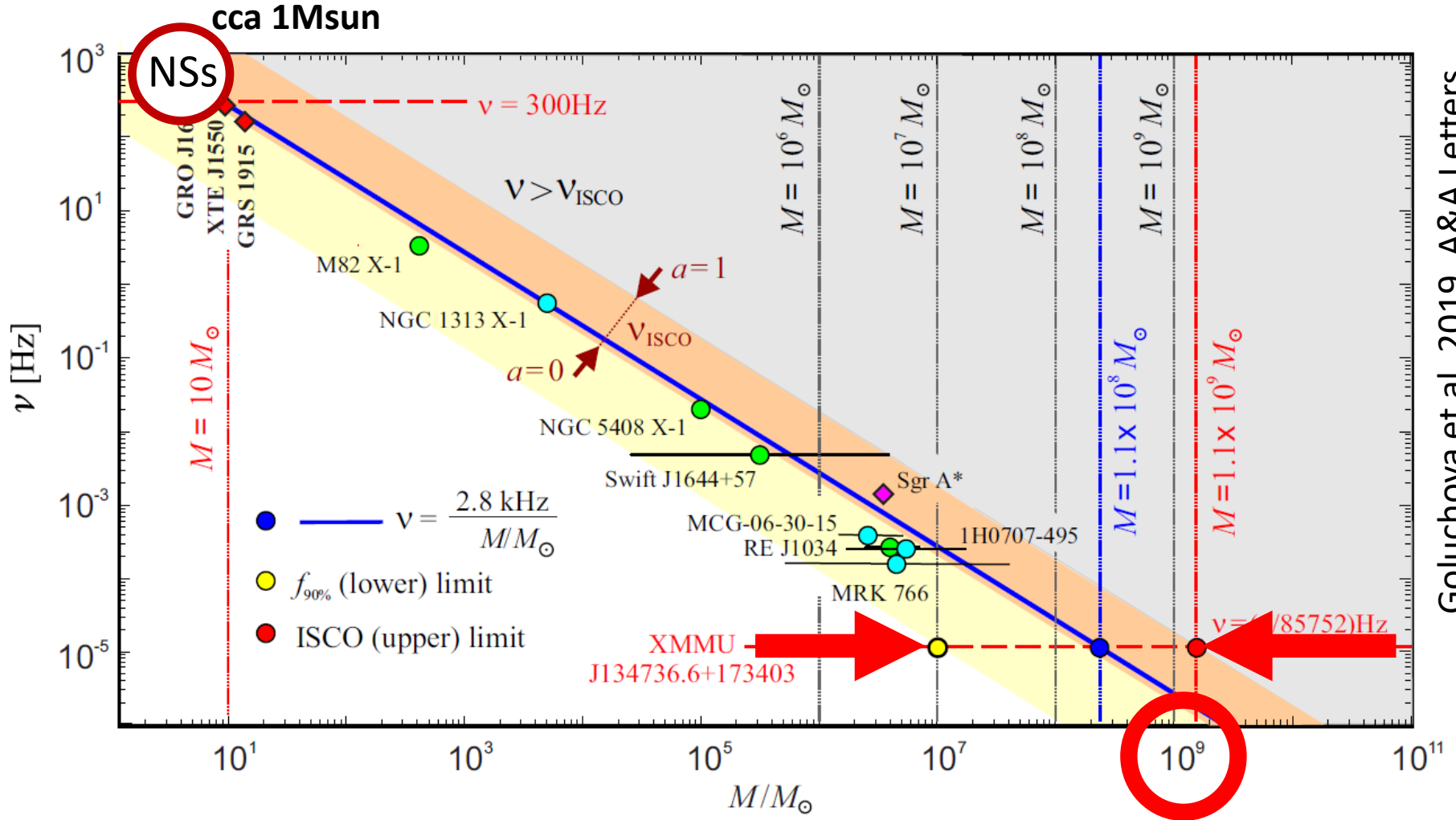
LMXBs provide a unique chance to probe effects in the strong-gravity-field region. The way how electromagnetic radiation propagates in space, its time variability and shape of lines in its energetic spectrum are invaluable probes to physical behavior of the matter in strong gravitational field. Similarly, a systematic study of the properties of neutron stars allows us to explore supradense matter.



VAN DER KLIS ET AL. 1997

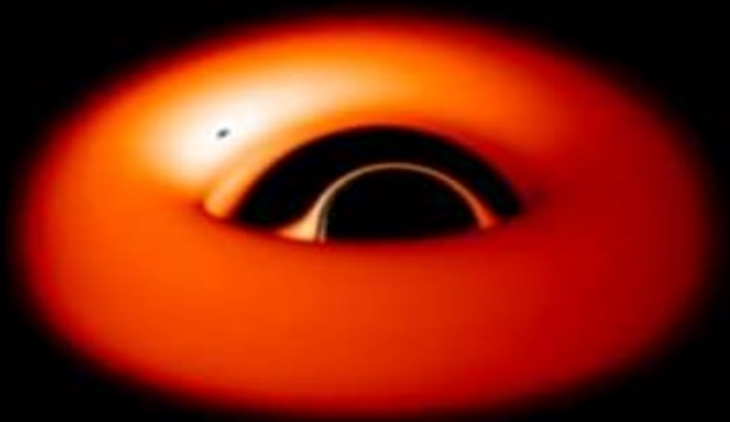
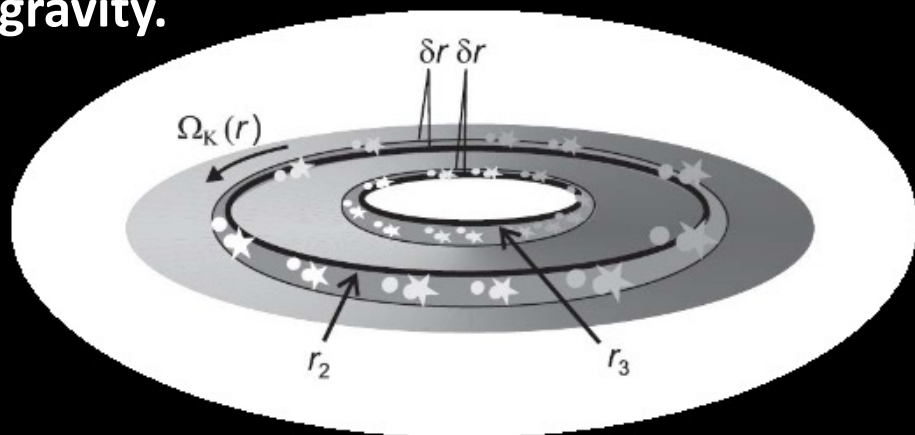
1. Rapid variability of accreting compact objects, HF QPOs and GR

There is a large variety of ideas proposed to explain the QPO phenomenon. Most often the QPOs are related to orbital motion in strong gravity. Indeed, the QPO frequencies (seem to) follow relativistic $1/M$ scaling.



1. Rapid variability of accreting compact objects, HF QPOs and GR

There is a large variety of ideas proposed to explain the HF QPO phenomenon. Most often the QPOs are related to orbital motion in strong gravity.



“Local oscillations”

RP model (Stella),
TD model (Cadez),
....

RP

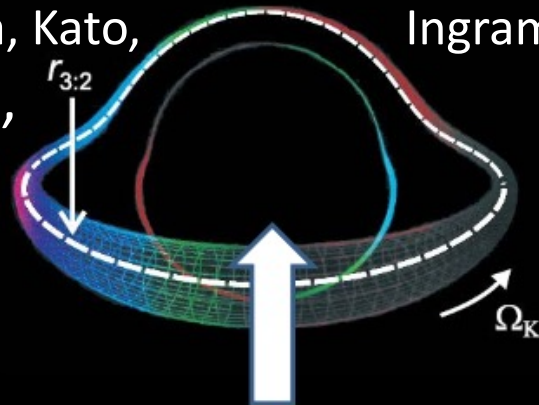


TD



“Global oscillations”

ER model (Abramowicz & Kluzniak),
p-modes, c-modes,... (Wagoner,
Rezzolla, Kato, Ingram,
Done...),
....



2. Twin peak QPOs and their models

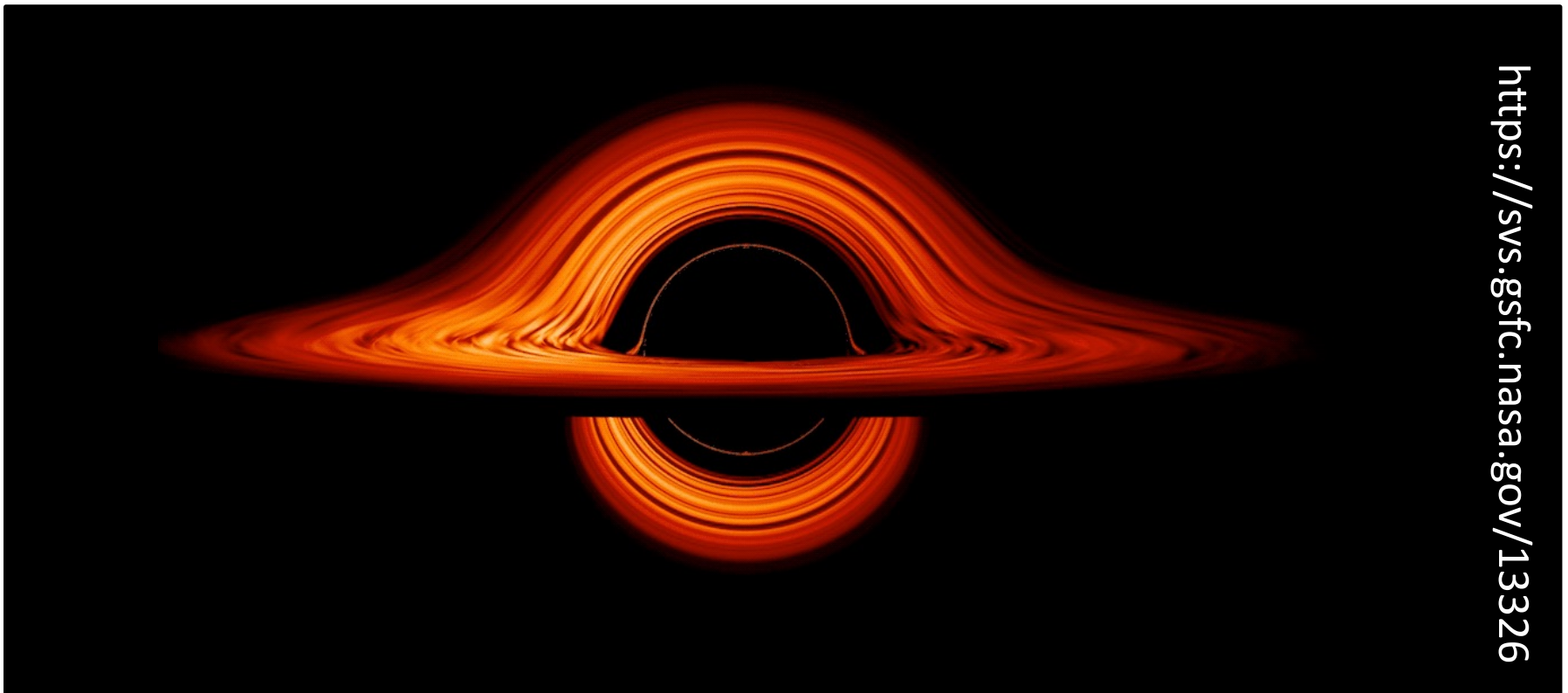


In the following we focus namely on

- Neutron star (twin peak) QPOs, atoll sources

▶ **Keplerian motion and relativistic precession model (RP model)**

- Stella et al. 1999, Kluzniak et al. 1992: clumps orbiting close to ISCO



<https://svs.gsfc.nasa.gov/13326>

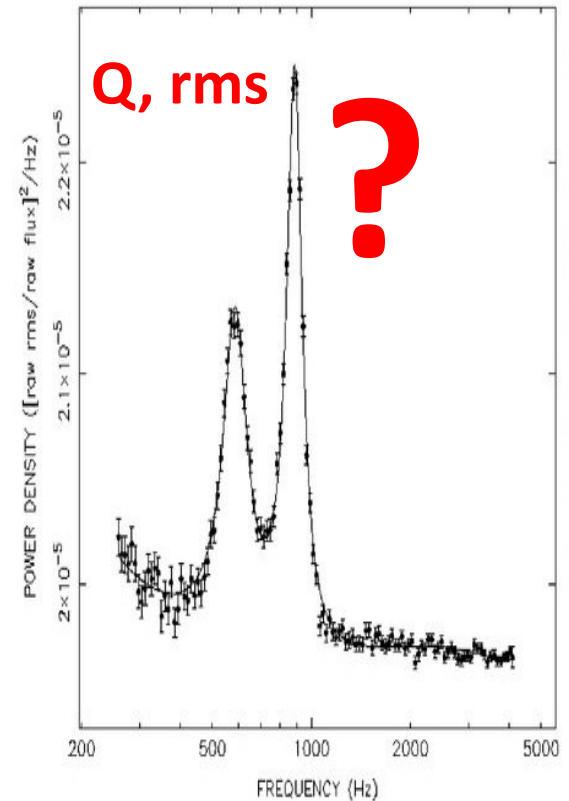
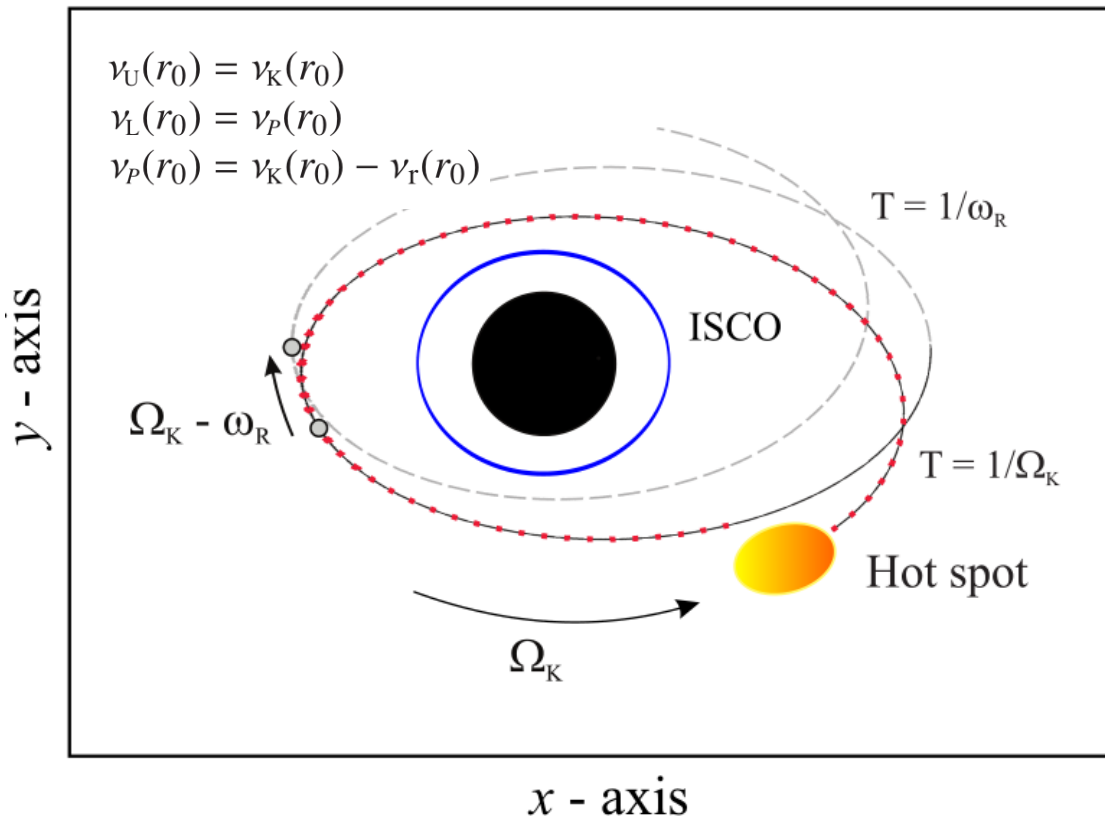
2. Twin peak QPOs and their models

In the following we focus namely on

- Neutron star (twin peak) QPOs, atoll sources

Keplerian motion and relativistic precession model (RP model)

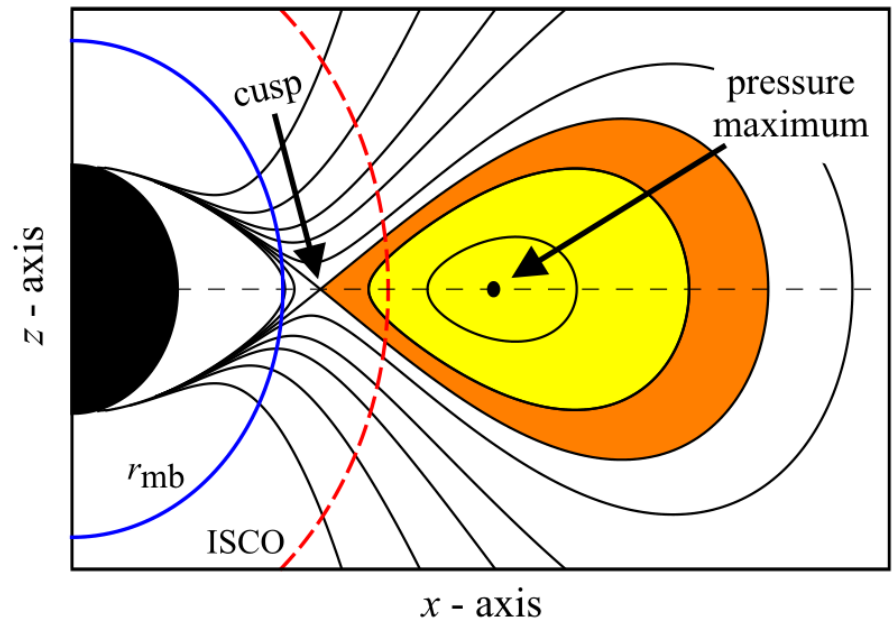
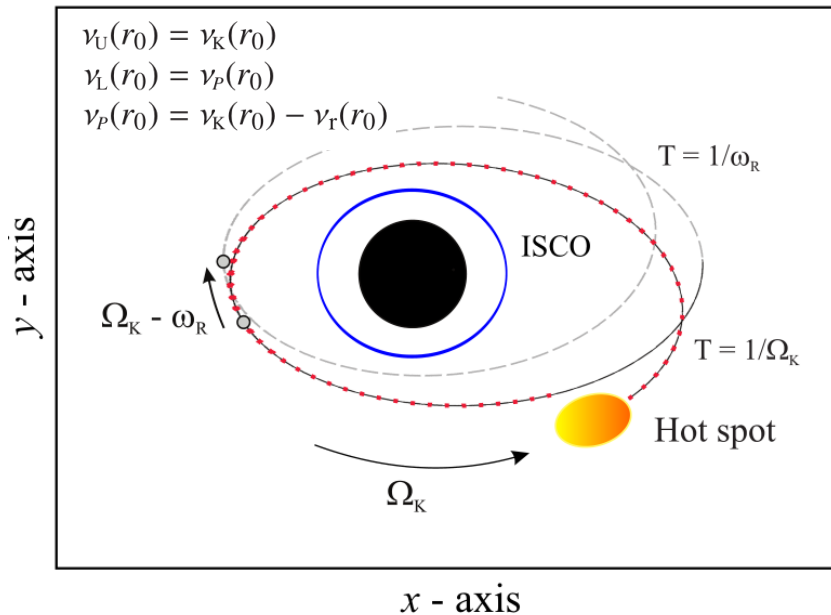
- Stella et al. 1999, Kluzniak et al. 1992: clumps orbiting close to ISCO



2. Twin peak QPOs and their models

In the following we focus namely on

- Neutron star (twin peak) QPOs, atoll sources
 - Keplerian motion and relativistic precession model (RP model)
- ➔ **Epicyclic modes consideration** that may serve as a plausible alternative to RP model – in general, consideration of the global motion of the fluid pose a much higher potential to explain high amplitudes and coherence times of QPOs observed in neutron star sources.

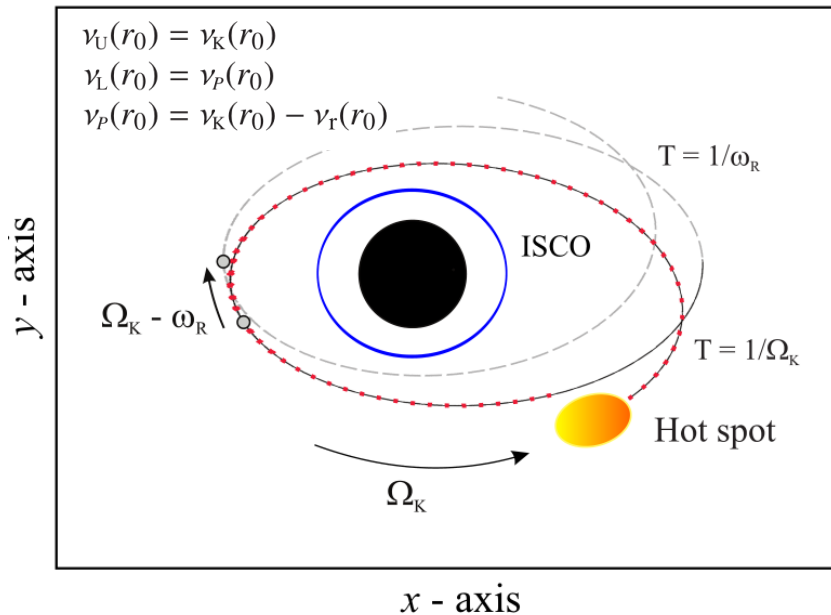


2. Twin peak QPOs and their models

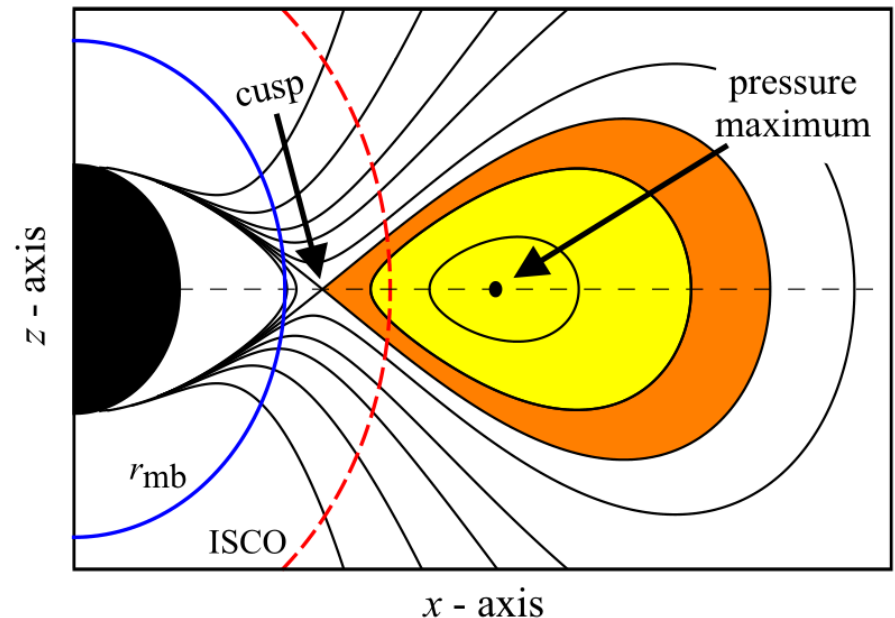
In the following we focus namely on

- Neutron star (twin peak) QPOs, atoll sources
- Keplerian motion and relativistic precession model (RP model)
- Epicyclic modes consideration

➔ **RP model:**
local geodesic precession

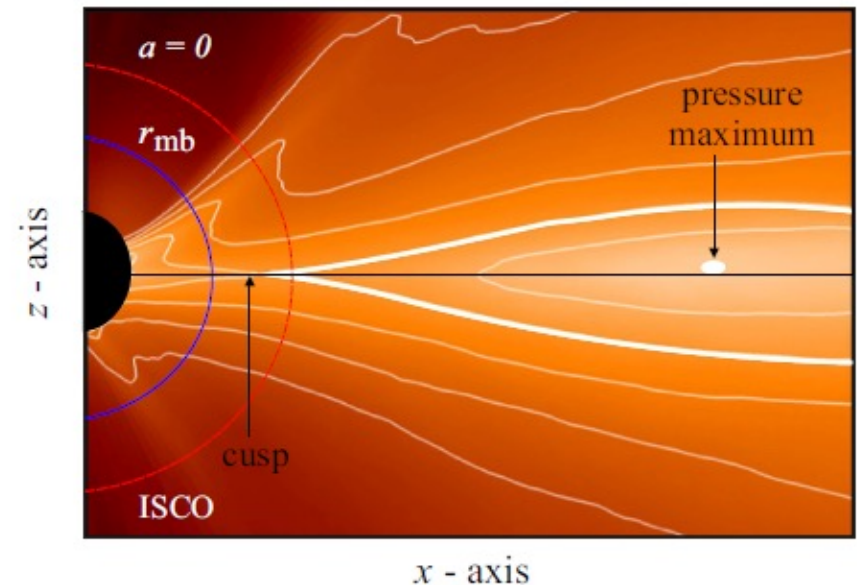
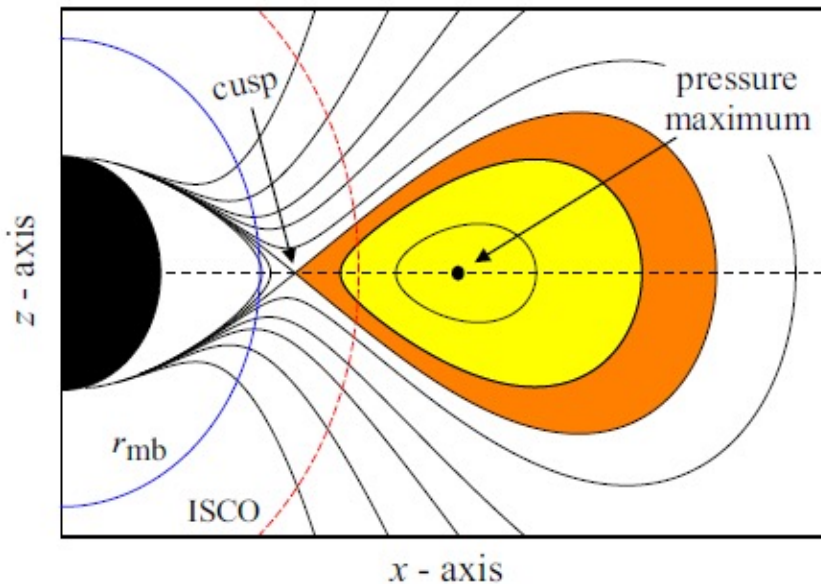


➔ **CT model:**
precession of the fluid flow



3. NS QPOs and epicyclic modes in non-slender torus (CT model)

The CT model has been suggested as the RP model alternative which deals with torus oscillations. It is based on the expectation that cusp configurations are likely to appear in real accretion flows, in which case the actual overall accretion rate through the inner edge of the disk can be strongly modulated by the disk oscillations.



Mode identification: radial precession mode, Keplerian motion.

4. Simple analytic formula relating mass and spin to QPOs ($j = 0$)

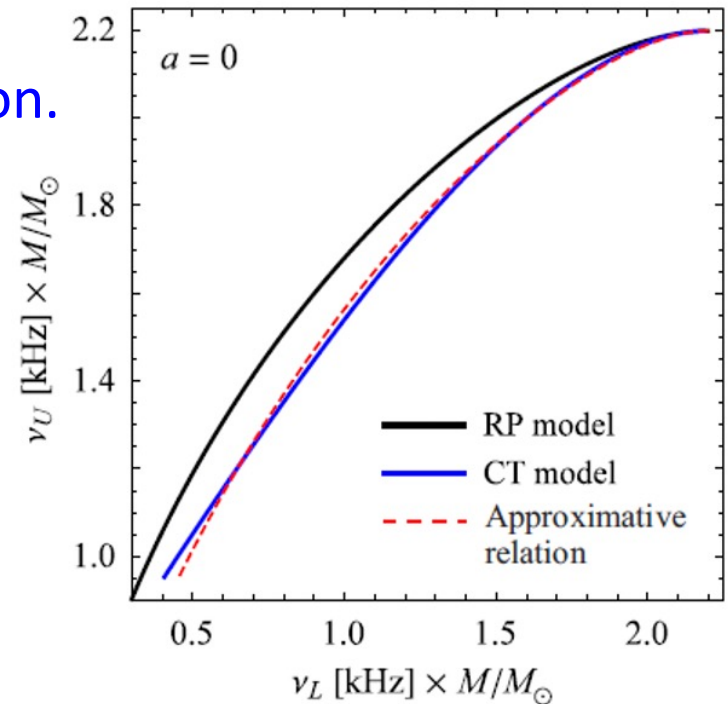
The relation between QPO frequencies predicted by CT model are implicitly given by a long set of formulae that have to be solved numerically (even for non-rotating stars, $j=0$).

BUT there is a very accurate approximation.

$$\nu_L = \nu_U \left(1 - \mathcal{B} \sqrt{1 - (\nu_U/\nu_0)^{2/3}} \right),$$

$$\nu_0 = \mathcal{F} \frac{1}{6^{3/2}}, \quad \mathcal{F} \equiv c^3 / (2\pi GM).$$

- When we assume $j=0$,
- $B=1$ corresponds to the exact prediction of RP model while
- $B=0.8$ well mimics the CT model prediction.




4. Simple analytic formula: Hartle-Thorne

$$\nu_L = \nu_U \left[1 - \mathcal{B} \sqrt{1 + 8j\mathcal{V}_0 - 6\mathcal{V}_0^{2/3} - Q\mathcal{V}_0^{4/3}} \right]$$

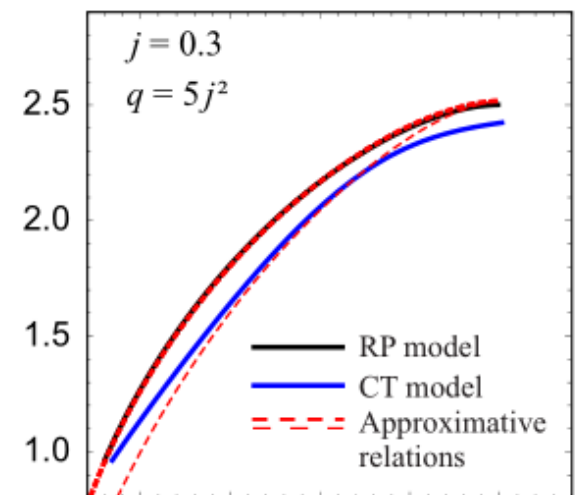
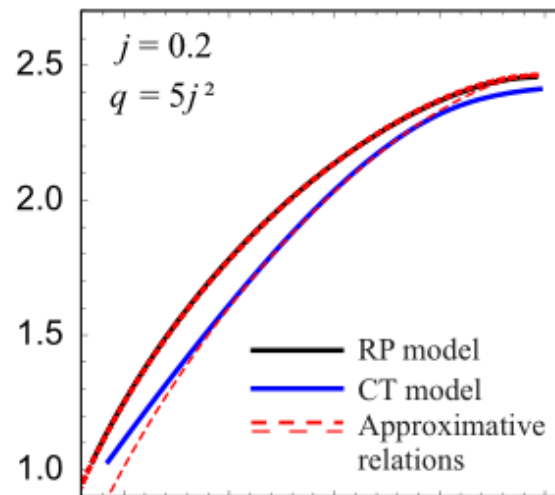
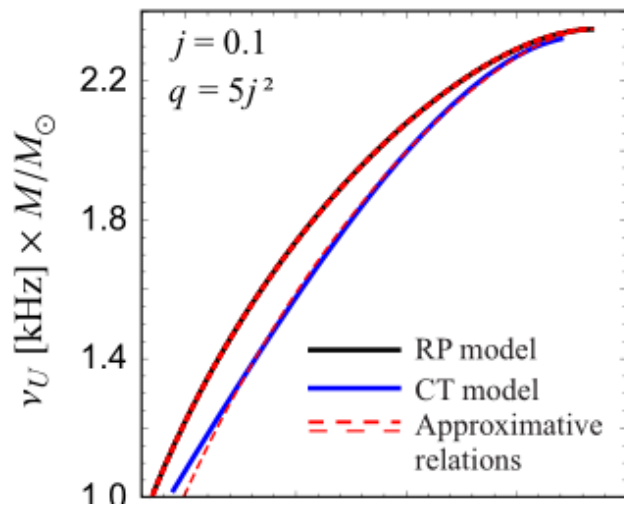
where

$$\mathcal{V}_0 \equiv \frac{\nu_U/\nu_0}{6^{3/2} - j\nu_U/\nu_0}, \quad \nu_0 = 2198 \frac{M_\odot}{M}, \quad Q = \frac{1}{3}(8j^2 - 17q)$$



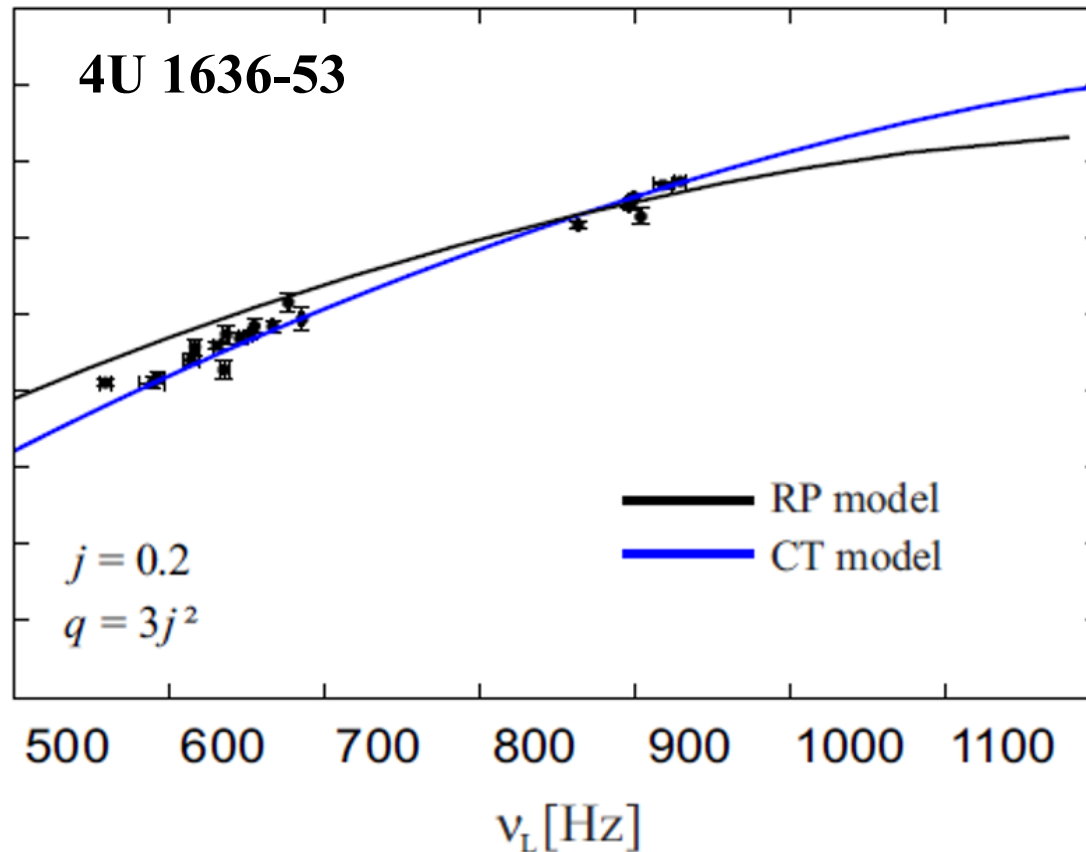
RP model:
 $\mathcal{B} = 1$

CT model:
 $\mathcal{B} = 0.8 - 0.2j$



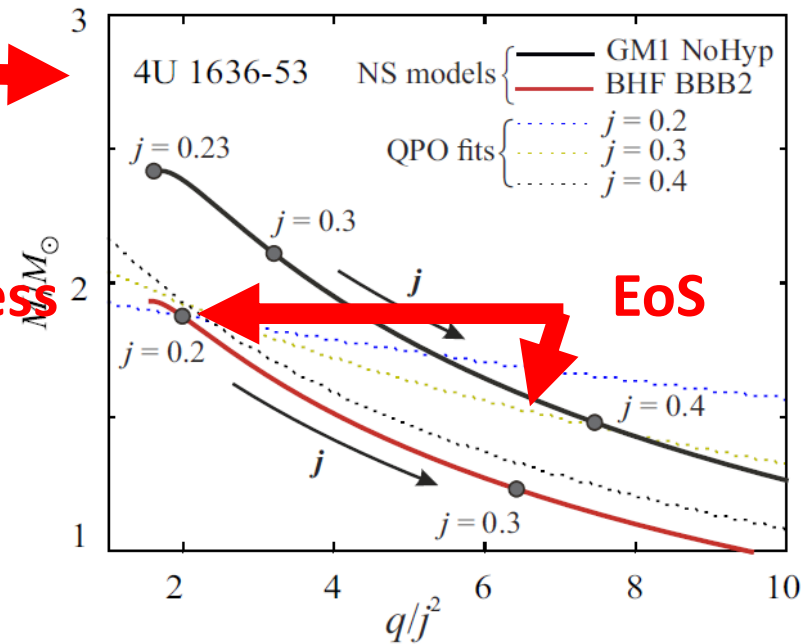
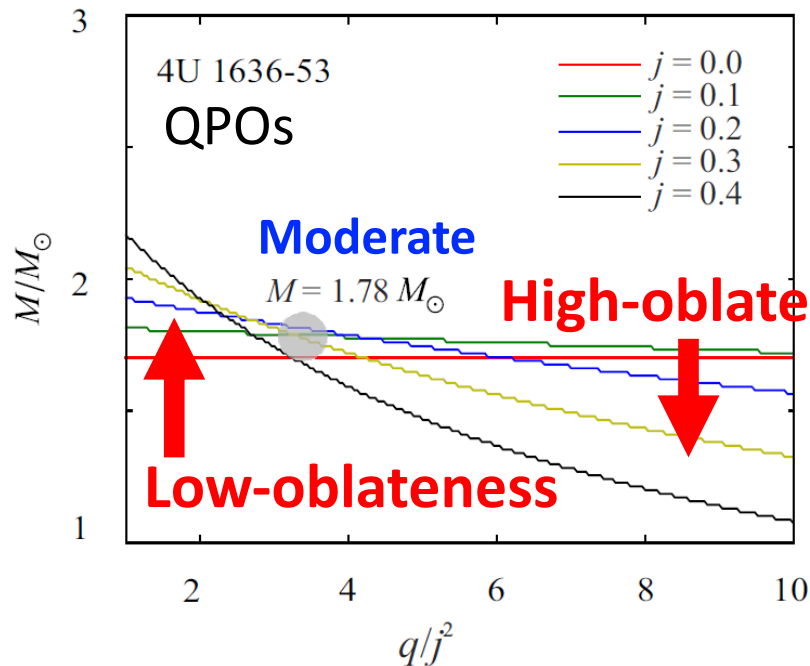
5. Application of our formula on 4U 1636-53

We find that, in HT spacetimes, the CT model provides generally better fits of the NS data than the RP model. It also predicts a lower NS mass than the RP model. *Note that, for the both simplified models, there is the same given fixed number of free parameters (degrees of freedom).*



5. Application of our formula on 4U 1636-53: mass, EoS (spin 581Hz)

- The implications based on QPOs can be faced to NS models assuming the spin frequency of 580Hz inferred from X-ray bursts.
- Several EoS can be excluded, but various modern EoS matches the data well.
- We arrive at the NS mass about 1.7-1.9 Solar masses for any EoS which matches the data well.



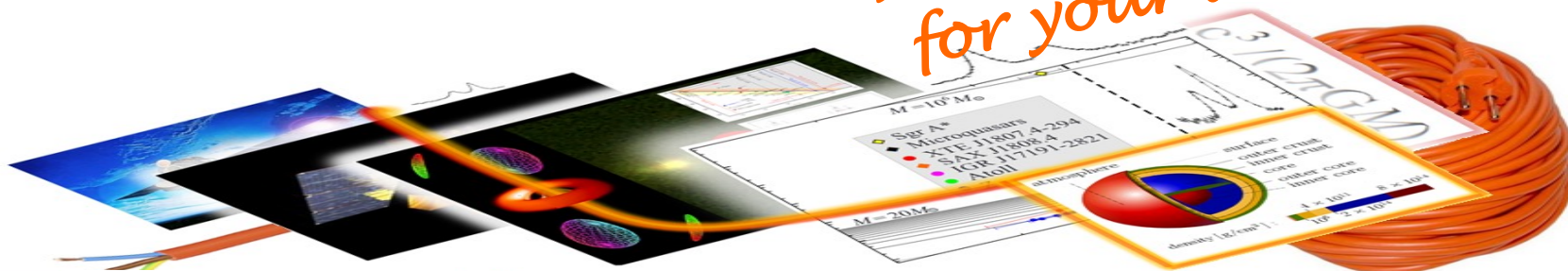
6. Conclusions (NSs)

The consideration of fluid precession (CT model) provides better fits of the data than the consideration of geodesic precession (RP model). The model predicts a lower NS mass than the RP model.

(Torok et al. 2022, *Apj*; Klimovicova et al., in prep.).

Source	Mass [M_{\odot}]	Source	Mass [M_{\odot}]	Source	Mass [M_{\odot}]
4U 0614+09	1.78	4U 1608-52	1.9	4U 1636-53	1.75
4U 1728-34	1.63	4U 1735-44	1.78	4U 1820-30	1.9
4U 1915-05	1.63	IGR J17191-2821	1.63	XTE J1807.4-294	2.68
GX 5-1	1.69	GX 17+2	1.96	GX 340+0	1.66
Sco X-1	1.87				

Thank you
for your attention



EUROPEAN UNION
European Structural and Investment Funds
Operational Programme Research,
Development and Education

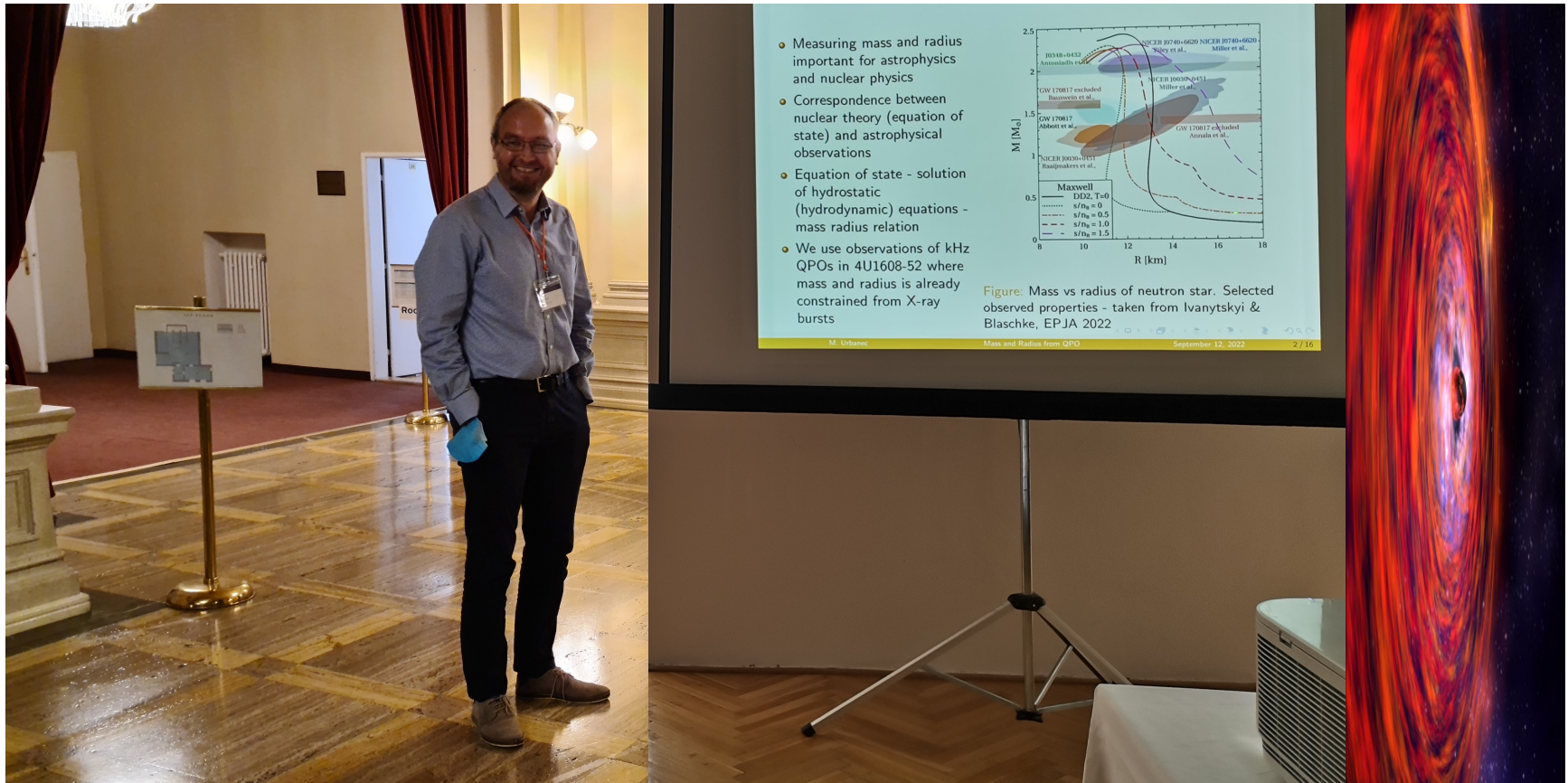


MINISTRY OF EDUCATION,
YOUTH AND SPORTS

GAČR No. 21-06825X

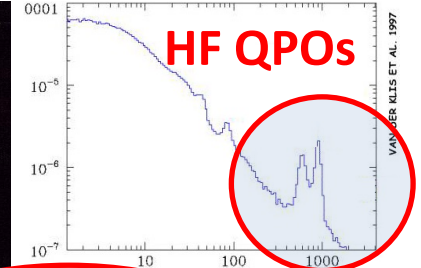
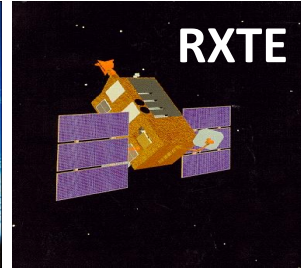
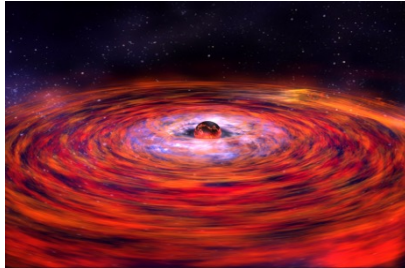
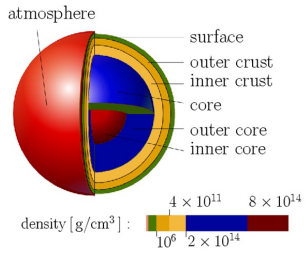
1. Rapid variability of accreting compact objects, HF QPOs and GR

LMXBs provide a unique chance to probe effects in the strong-gravity-field region. The way how electromagnetic radiation propagates in space, its time variability and shape of lines in its energetic spectrum are invaluable probes to physical behavior of the matter in strong gravitational field. Similarly, a systematic study of the properties of neutron stars allows us to explore supradense matter.



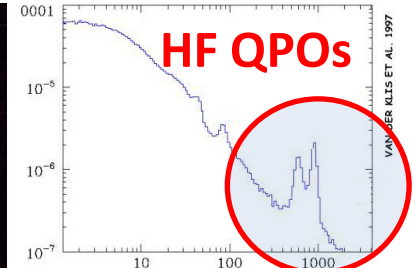
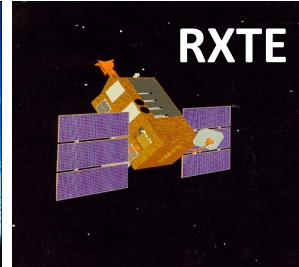
1. Rapid variability of accreting compact objects, HF QPOs and GR

LMXBs provide a unique chance to probe effects in the strong-gravity-field region. The way how electromagnetic radiation propagates in space, its time variability and shape of lines in its energetic spectrum are invaluable probes to physical behavior of the matter in strong gravitational field. Similarly, a systematic study of the properties of neutron stars allows us to explore supradense matter. But these systems are not optically resolved and the (degenerated) spectral or timing information could be somewhat confusing....




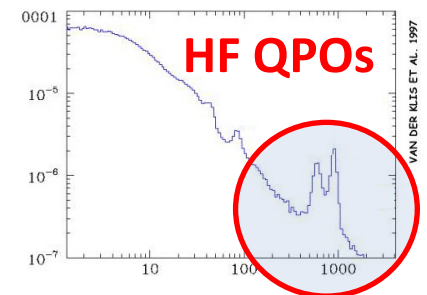
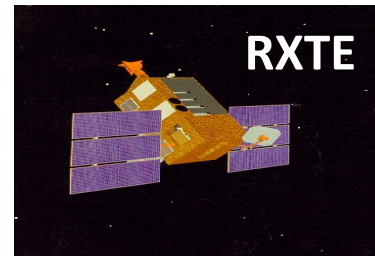
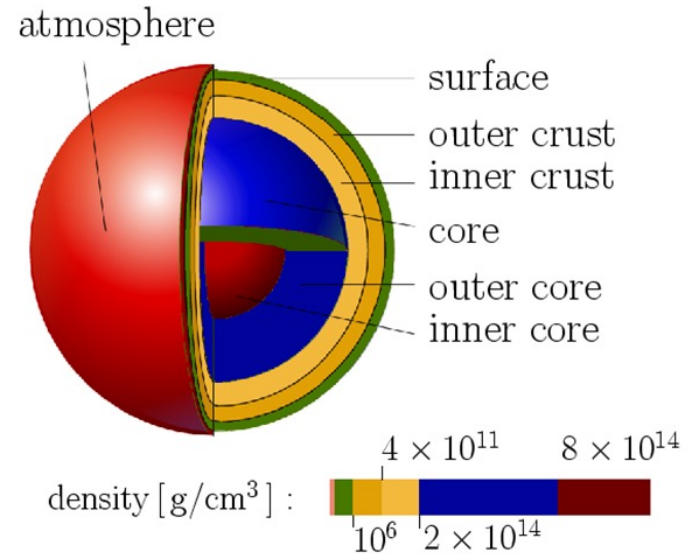
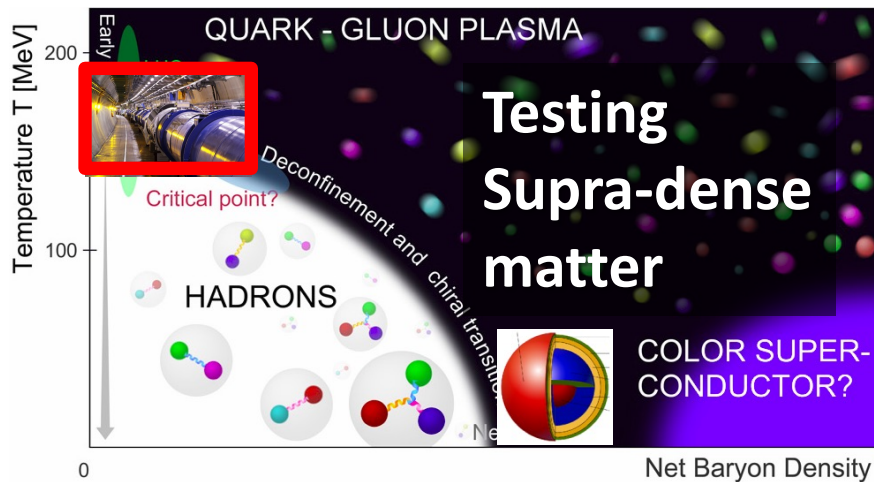
1. Rapid variability of accreting compact objects, HF QPOs and GR

LMXBs provide a unique chance to probe effects in the strong-gravity-field region. The way how electromagnetic radiation propagates in space, its time variability and shape of lines in its energetic spectrum are invaluable probes to physical behavior of the matter in strong gravitational field. Similarly, a systematic study of the properties of neutron stars allows us to explore supradense matter. But these systems are not optically resolved and the (degenerated) spectral or timing information could be somewhat confusing....



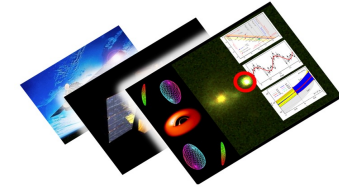
1. Rapid variability of accreting compact objects, HF QPOs and GR

Despite , accreting BHs and NSs provide a unique chance to probe effects in the strong-gravity-field region. The way how electromagnetic radiation propagates in space, its time variability and shape of lines in its energetic spectrum are invaluable probes to physical behavior of the matter in strong gravitational field. Similarly, a systematic study of the properties of neutron stars allows us to explore supradense matter.

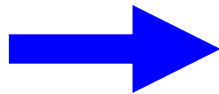


1. Rapid variability of accreting compact objects, HF QPOs and GR

- *There is robust evidence for the large range $1/M$ scaling of (X-ray HF) QPOs – from NSs & microquasars to XMM BH.*

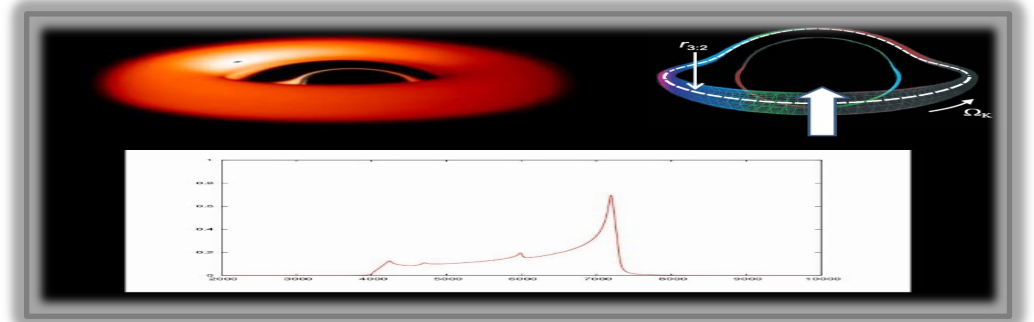


- *The measured frequency provides an upper limit on M when the ISCO frequency is considered. The lower limit can be inferred as well when the disc emissivity is taken into account. Overall, the scaling extends from microquasars to (Goluchova et al., A&A Letters, 2019)*



$$10^7 \text{ Msun} < M < 10^9 \text{ Msun.}$$

- *In NS sources we can identify characteristic periods of HF QPOs associated to individual sources. These possibly determine relative mass (spin) of each source within a given QPO model (Torok et al, MNRAS, 2019).*

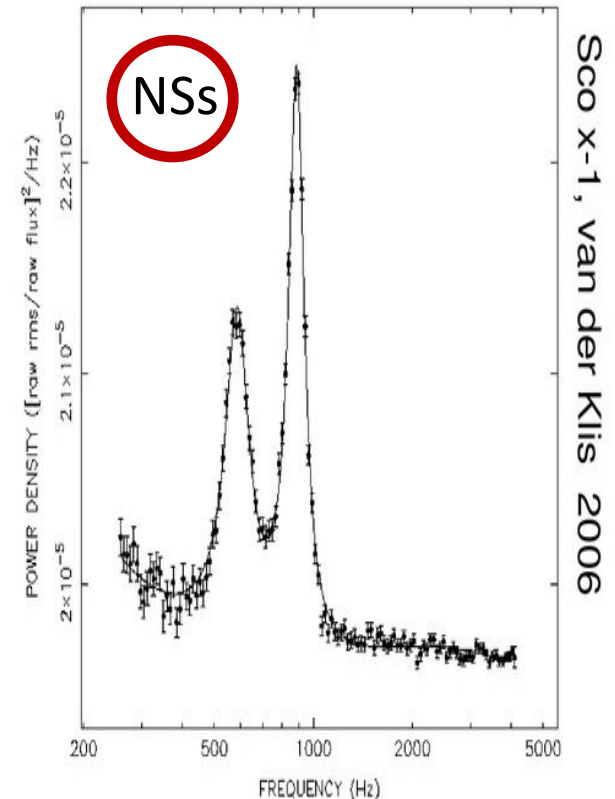
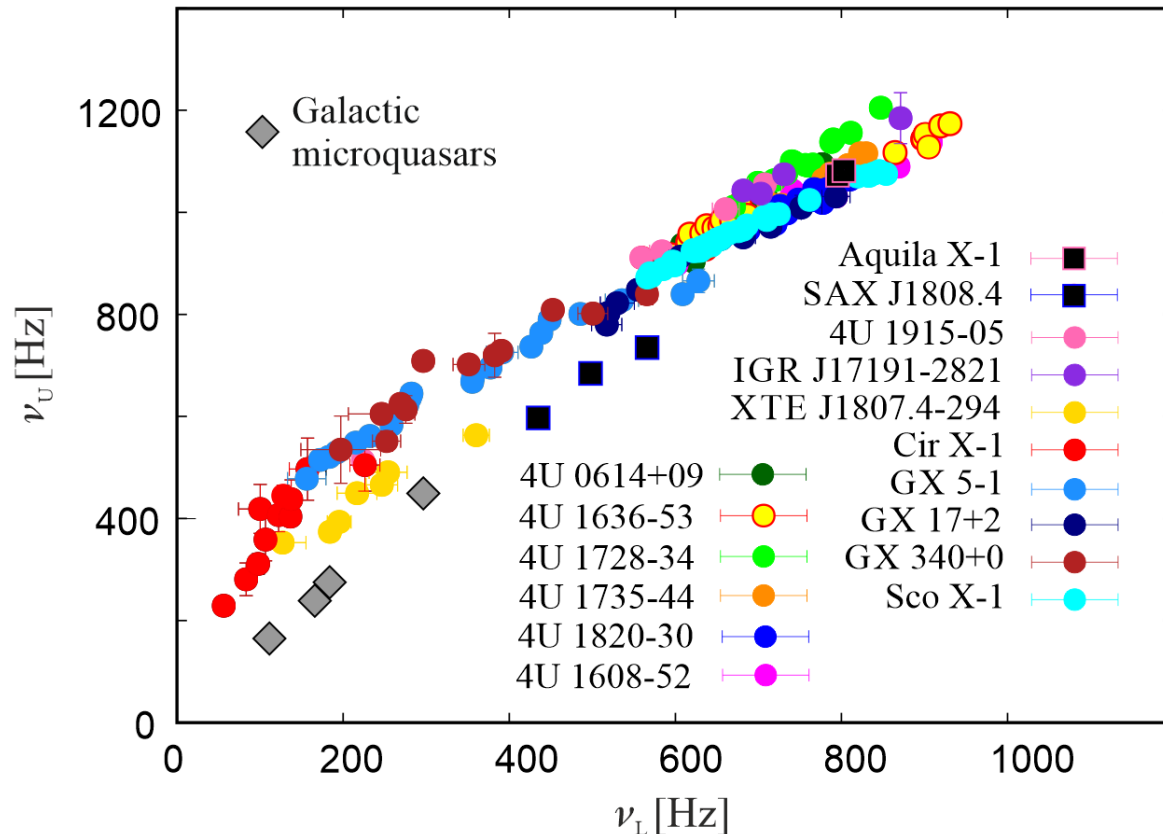


2. Twin peak QPOs and their models

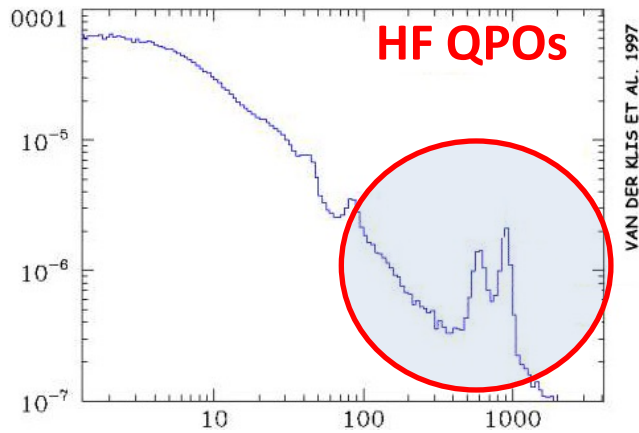
In the following we focus namely on

➔ **Neutron star (twin peak) QPOs, atoll sources**

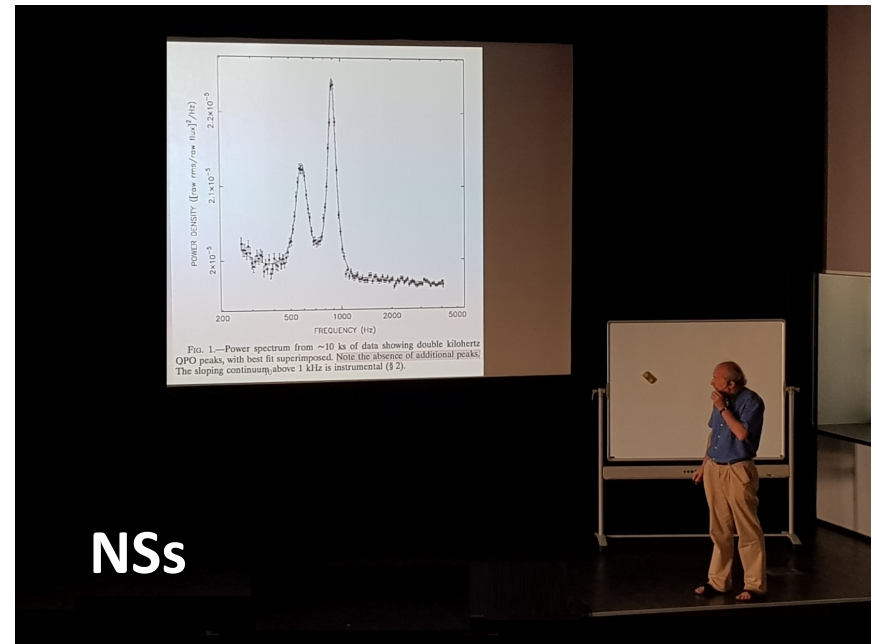
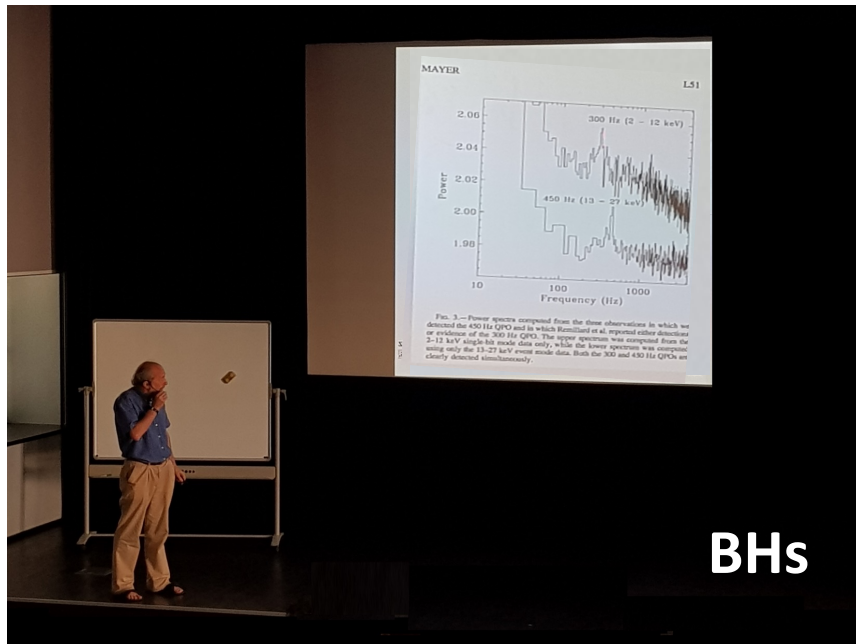
(low accretion rate, low magnetic field, very high QPO frequencies)



1. Rapid variability of accreting compact objects, HF QPOs and GR



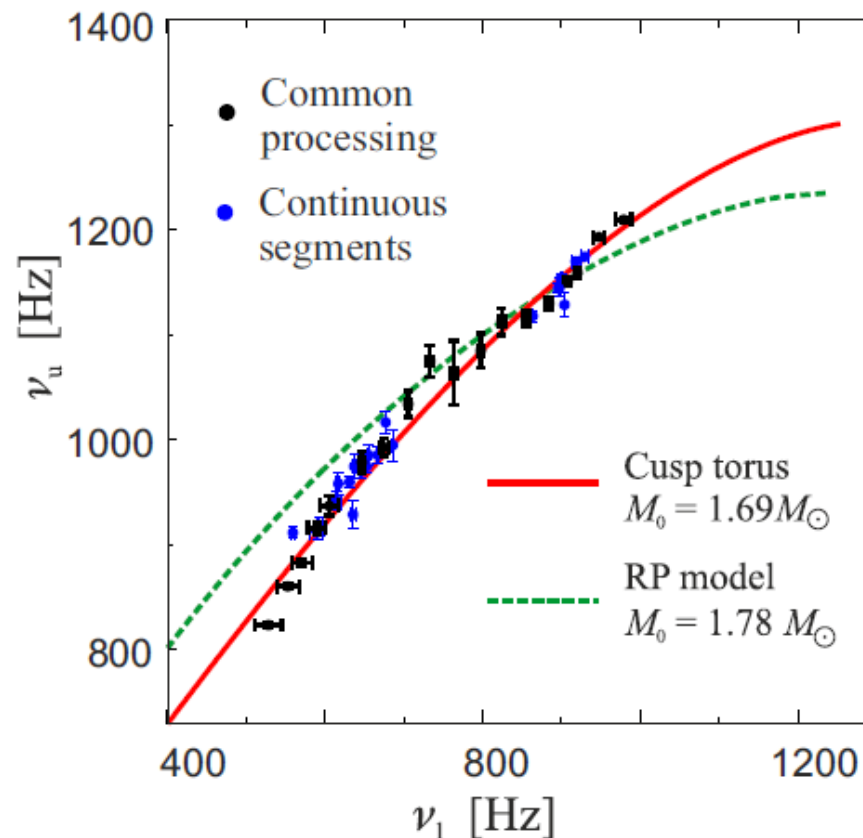
The high-frequency QPOs are observed in both BH and NS sources and span a frequency range of tens to more than thousands of Hertz. Their frequencies correspond to orbital frequencies in innermost parts of the accretion disk.



3. NS QPOs and epicyclic modes in non-slender torus (CT model)


The CT model provides generally better fits of the NS data than the RP model. It also predicts a lower NS mass than the RP model. *For the both simplified models, there is the same given fixed number of free parameters (degrees of freedom).*

Atoll source 4U 1636-53 (Torok et al., 2016 MNRAS L):




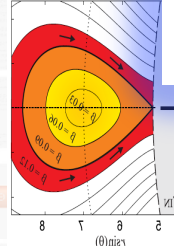
4. Simple analytic formula: Hartle-Thorne

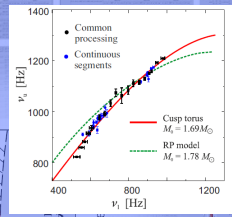
The relation between QPO frequencies predicted by CT model are implicitly given by a long set of formulae that have to be solved numerically...


$M, r,$
 (beta)
 $j,$
 q

computationally expensive









4. Simple analytic formula relating mass and spin to QPOs

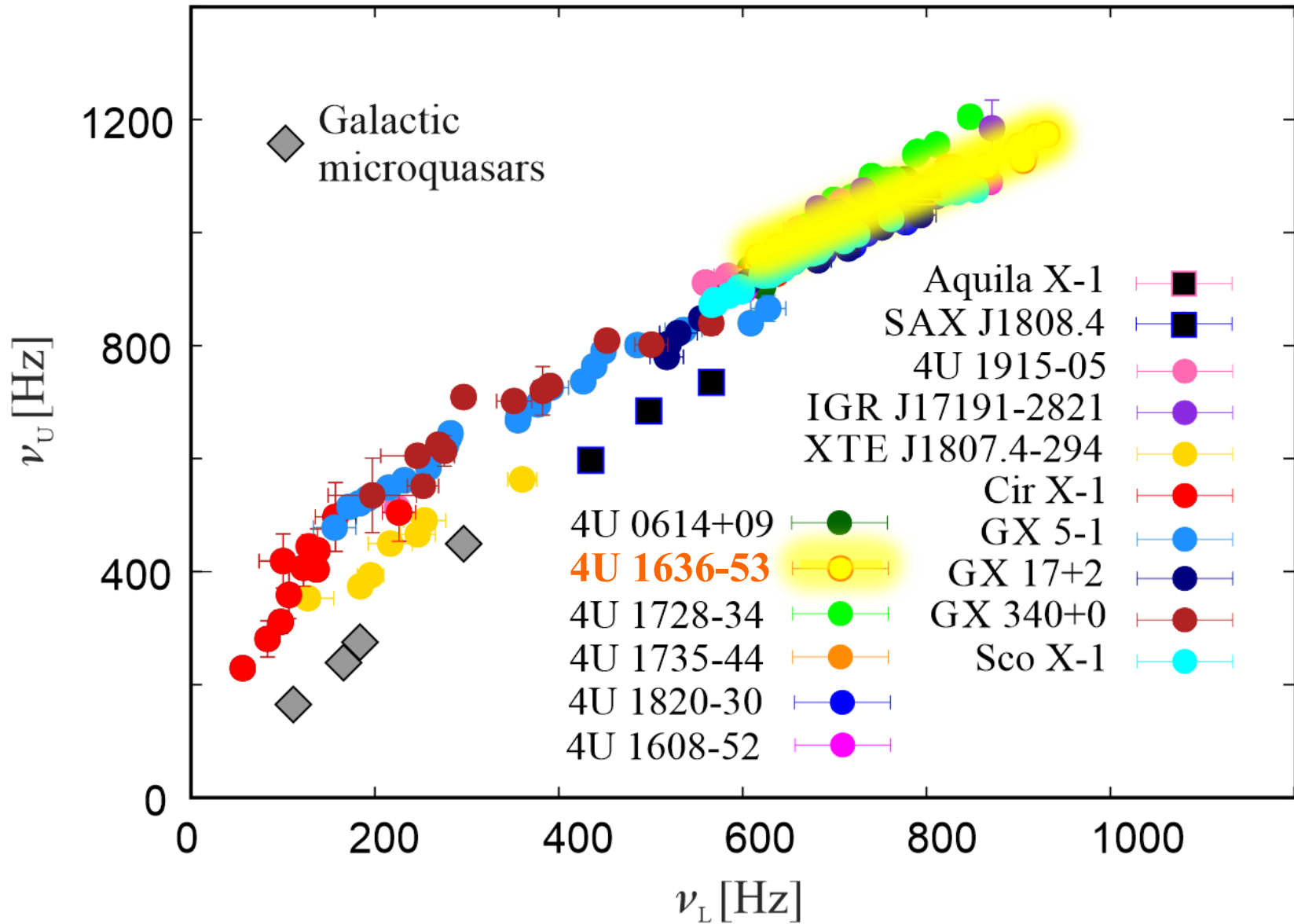
- The relation between QPO frequencies predicted by CT model are implicitly given by a long set of formulae that have to be solved numerically (**even for non-rotating stars, $j=0$**).

$M, r,$
 (β)

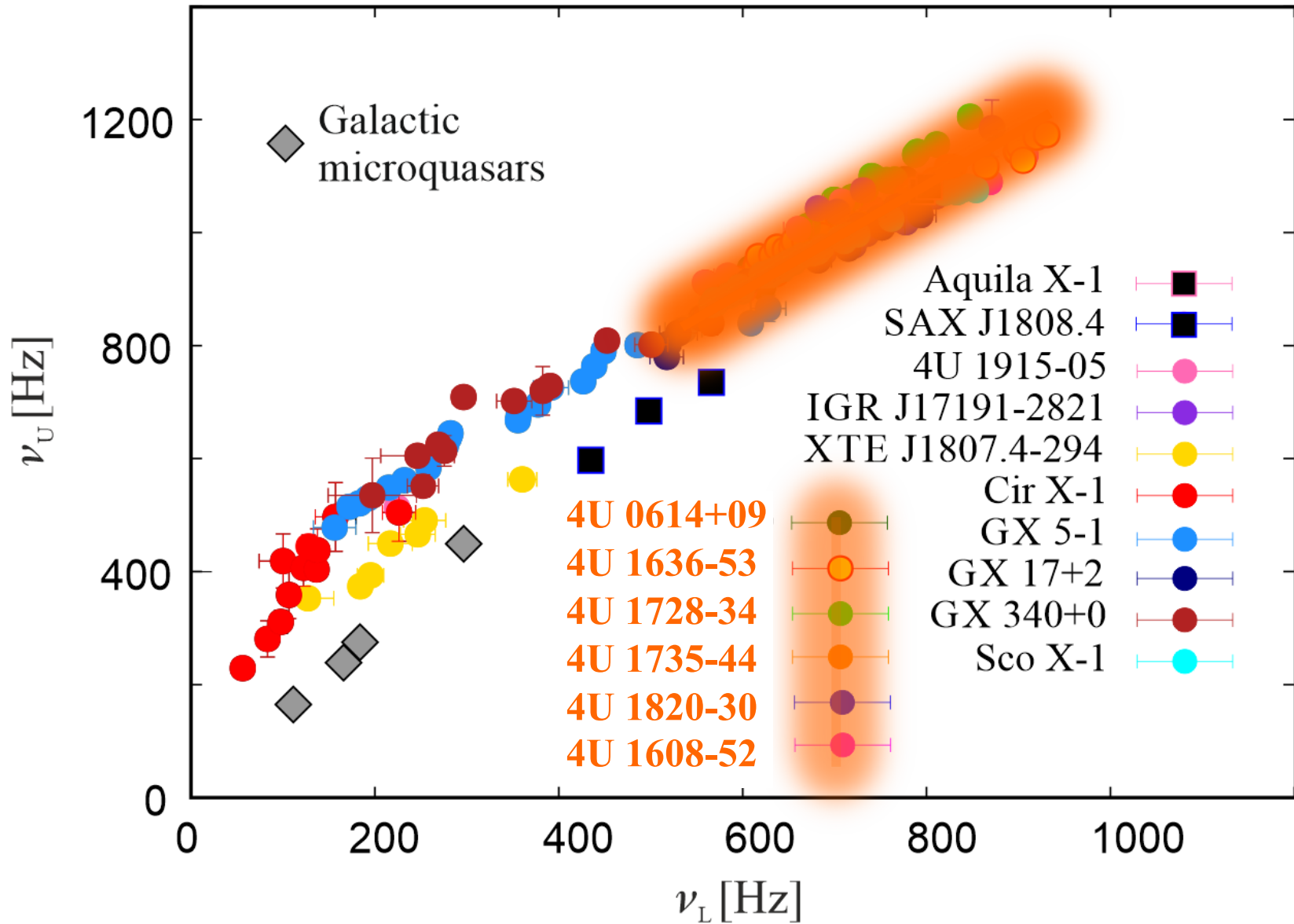
radial mode
frequency:

$$\begin{aligned}
 & r\theta^3 - 1.56922 \times 10^{26} r\theta^4 + \left(8.82939 \times 10^{25} + 3.17564 \times 10^9 \sqrt{4. + \frac{1764.}{r\theta^2} - \frac{24.}{r\theta}} \right) r\theta^5 + \\
 & 311 \times 10^8 \sqrt{4. + \frac{1764.}{r\theta^2} - \frac{24.}{r\theta}} r\theta^7 + \left(-8.7656 \times 10^{23} + 3.30796 \times 10^8 \sqrt{4. + \frac{1764.}{r\theta^2} - \frac{24.}{r\theta}} \right) r\theta^8 + \left(-3.06864 \times 10^{23} - 4.54845 \times 10^7 \sqrt{4. + \frac{1764.}{r\theta^2} - \frac{24.}{r\theta}} \right) r\theta^9 + \\
 & 10^6 \sqrt{4. + \frac{1764.}{r\theta^2} - \frac{24.}{r\theta}} r\theta^{10} + \left(-4.86063 \times 10^{22} + 193.826. \sqrt{4. + \frac{1764.}{r\theta^2} - \frac{24.}{r\theta}} \right) r\theta^{11} + \left(8.85192 \times 10^{21} - 60247.2 \sqrt{4. + \frac{1764.}{r\theta^2} - \frac{24.}{r\theta}} \right) r\theta^{12} + \left(-1.15737 \times 10^{21} - 5568.08 \sqrt{4. + \frac{1764.}{r\theta^2} - \frac{24.}{r\theta}} \right) r\theta^{13} + \\
 & \left(1.10779 \times 10^{20} - 1177.1 \sqrt{4. + \frac{1764.}{r\theta^2} - \frac{24.}{r\theta}} \right) r\theta^{14} + \left(-7.77278 \times 10^{18} + 43.3774 \sqrt{4. + \frac{1764.}{r\theta^2} - \frac{24.}{r\theta}} \right) r\theta^{15} + \left(3.98163 \times 10^{17} - 0.492925 \sqrt{4. + \frac{1764.}{r\theta^2} - \frac{24.}{r\theta}} \right) r\theta^{16} + \left(-1.48033 \times 10^{16} - 0.246462 \sqrt{4. + \frac{1764.}{r\theta^2} - \frac{24.}{r\theta}} \right) r\theta^{17} + \\
 & \left(3.83911 \times 10^{14} + 0.00577646 \sqrt{4. + \frac{1764.}{r\theta^2} - \frac{24.}{r\theta}} \right) r\theta^{18} + \left(-5.47894 \times 10^{12} - 0.00114326 \sqrt{4. + \frac{1764.}{r\theta^2} - \frac{24.}{r\theta}} \right) r\theta^{19} + \left(-0.000236925 - 0.0000300857 \sqrt{4. + \frac{1764.}{r\theta^2} - \frac{24.}{r\theta}} \right) r\theta^{20} + 3.70196 \times 10^{-6} r\theta^{21} \beta^2 + \\
 & m \left(-2.84461 \times 10^{26} + 3.55576 \times 10^{26} \beta^2 + \left(-0.00047385 + 0.000179104 \sqrt{4. + \frac{1764.}{r\theta^2} - \frac{24.}{r\theta}} \right) r\theta^{21} \beta^2 + \left(0.0000296156 - 5.40603 \times 10^{-6} \sqrt{4. + \frac{1764.}{r\theta^2} - \frac{24.}{r\theta}} \right) r\theta^{22} \beta^2 + r\theta^6 \left(-8.94226 \times 10^{26} + \left(1.37548 \times 10^{27} - 7.80474 \times 10^{10} \sqrt{4. + \frac{1764.}{r\theta^2} - \frac{24.}{r\theta}} \right) \beta^2 \right) + \\
 & r\theta \left(1.3195 \times 10^{27} - \left(-1.70034 \times 10^{27} - 1.23881 \times 10^{10} \sqrt{4. + \frac{1764.}{r\theta^2} - \frac{24.}{r\theta}} \right) \beta^2 \right) + r\theta^8 \left(-6.7537 \times 10^{25} + \left(1.13463 \times 10^{26} - 9.69034 \times 10^9 \sqrt{4. + \frac{1764.}{r\theta^2} - \frac{24.}{r\theta}} \right) \beta^2 \right) + r\theta^9 \left(8.74457 \times 10^{24} + \left(-1.57904 \times 10^{25} - 8.27803 \times 10^8 \sqrt{4. + \frac{1764.}{r\theta^2} - \frac{24.}{r\theta}} \right) \beta^2 \right) + \\
 & r\theta^{12} \left(1.29352 \times 10^{23} + \left(-2.33747 \times 10^{23} - 2.92688 \times 10^7 \sqrt{4. + \frac{1764.}{r\theta^2} - \frac{24.}{r\theta}} \right) \beta^2 \right) + r\theta^{14} \left(2.59926 \times 10^{21} + \left(-5.04296 \times 10^{21} - 294.766. \sqrt{4. + \frac{1764.}{r\theta^2} - \frac{24.}{r\theta}} \right) \beta^2 \right) + r\theta^{16} \left(1.47164 \times 10^{19} + \left(-3.0004 \times 10^{19} - 1640.92 \sqrt{4. + \frac{1764.}{r\theta^2} - \frac{24.}{r\theta}} \right) \beta^2 \right) + \\
 & r\theta^{18} \left(2.46352 \times 10^{16} + \left(-5.19971 \times 10^{16} - 5.58581 \sqrt{4. + \frac{1764.}{r\theta^2} - \frac{24.}{r\theta}} \right) \beta^2 \right) + r\theta^{20} \left(7.71681 \times 10^{12} + \left(-1.6977 \times 10^{13} - 0.0078002 \sqrt{4. + \frac{1764.}{r\theta^2} - \frac{24.}{r\theta}} \right) \beta^2 \right) + r\theta^{19} \left(-5.95738 \times 10^{14} + \left(1.28053 \times 10^{15} + 0.26287 \sqrt{4. + \frac{1764.}{r\theta^2} - \frac{24.}{r\theta}} \right) \beta^2 \right) + \\
 & r\theta^{17} \left(-7.03983 \times 10^{17} + \left(1.46195 \times 10^{18} + 131.742 \sqrt{4. + \frac{1764.}{r\theta^2} - \frac{24.}{r\theta}} \right) \beta^2 \right) + r\theta^{15} \left(-2.27399 \times 10^{20} + \left(4.53297 \times 10^{20} - 23.119.8 \sqrt{4. + \frac{1764.}{r\theta^2} - \frac{24.}{r\theta}} \right) \beta^2 \right) + r\theta^{13} \left(-2.17888 \times 10^{22} + \left(4.09415 \times 10^{22} + 3.93679 \times 10^6 \sqrt{4. + \frac{1764.}{r\theta^2} - \frac{24.}{r\theta}} \right) \beta^2 \right) + \\
 & r\theta^{11} \left(-4.77965 \times 10^{23} + \left(8.15222 \times 10^{23} + 1.6536 \times 10^7 \sqrt{4. + \frac{1764.}{r\theta^2} - \frac{24.}{r\theta}} \right) \beta^2 \right) + r\theta^{10} \left(3.37384 \times 10^{23} + \left(-3.40687 \times 10^{23} - 7.17066 \times 10^8 \sqrt{4. + \frac{1764.}{r\theta^2} - \frac{24.}{r\theta}} \right) \beta^2 \right) + \\
 & r\theta^4 \left(-3.16276 \times 10^{27} + \left(4.51052 \times 10^{27} + 1.48141 \times 10^{10} \sqrt{4. + \frac{1764.}{r\theta^2} - \frac{24.}{r\theta}} \right) \beta^2 \right) + r\theta^7 \left(2.95069 \times 10^{26} + \left(-4.72967 \times 10^{26} - 1.8858 \times 10^{10} \sqrt{4. + \frac{1764.}{r\theta^2} - \frac{24.}{r\theta}} \right) \beta^2 \right) + r\theta^2 \left(-2.80587 \times 10^{27} + \left(3.73392 \times 10^{27} + 3.80566 \times 10^{10} \sqrt{4. + \frac{1764.}{r\theta^2} - \frac{24.}{r\theta}} \right) \beta^2 \right) + \\
 & r\theta^3 \left(3.62136 \times 10^{27} + \left(-4.98493 \times 10^{27} + 6.36914 \times 10^{10} \sqrt{4. + \frac{1764.}{r\theta^2} - \frac{24.}{r\theta}} \right) \beta^2 \right) + r\theta^5 \left(1.96944 \times 10^{27} + \left(-2.91441 \times 10^{27} - 1.21376 \times 10^{11} \sqrt{4. + \frac{1764.}{r\theta^2} - \frac{24.}{r\theta}} \right) \beta^2 \right) + \\
 & \sqrt{\frac{-6 - r\theta}{r\theta}} \left(-2.84461 \times 10^{26} - 2.47718 \times 10^{26} \beta^2 + \left(0.000710776 - 0.000101451 \sqrt{4. + \frac{1764.}{r\theta^2} - \frac{24.}{r\theta}} \right) r\theta^{21} \beta^2 + \left(-0.0000296156 - 1.17522 \times 10^{-6} \sqrt{4. + \frac{1764.}{r\theta^2} - \frac{24.}{r\theta}} \right) r\theta^{22} \beta^2 \right)
 \end{aligned}$$

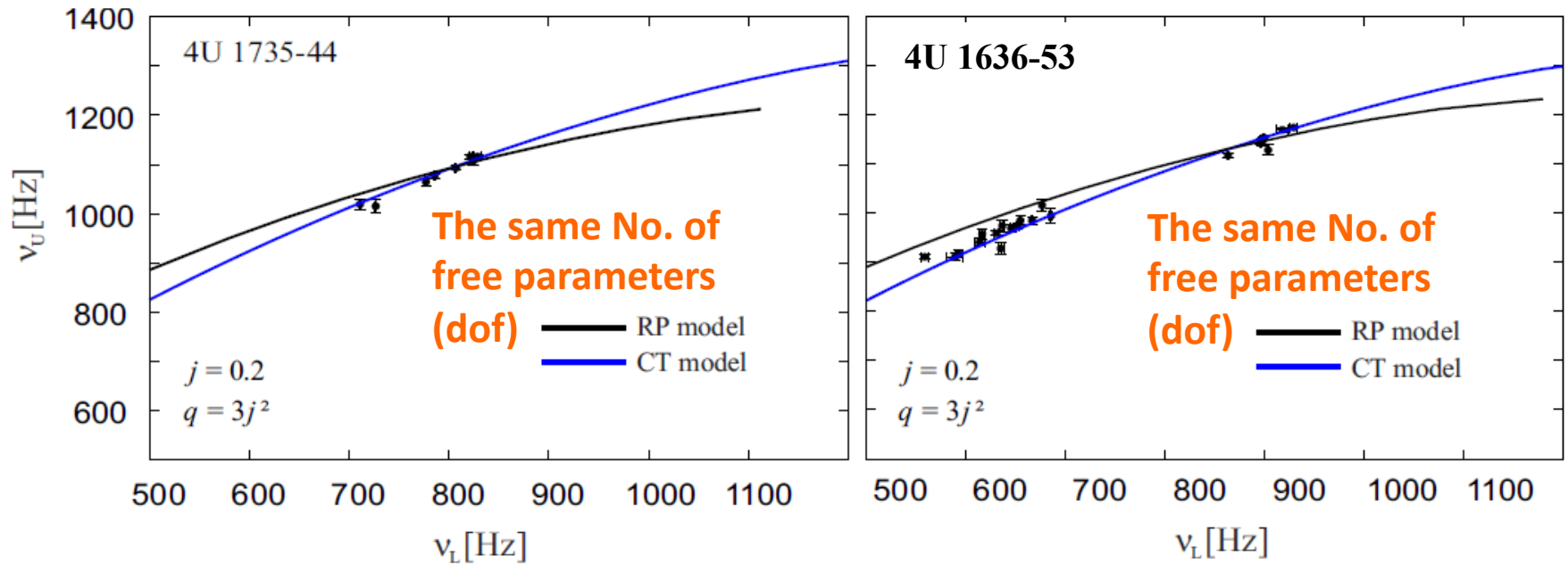
6. Conclusions (mass of atoll sources)



6. Conclusions (mass of atoll sources)



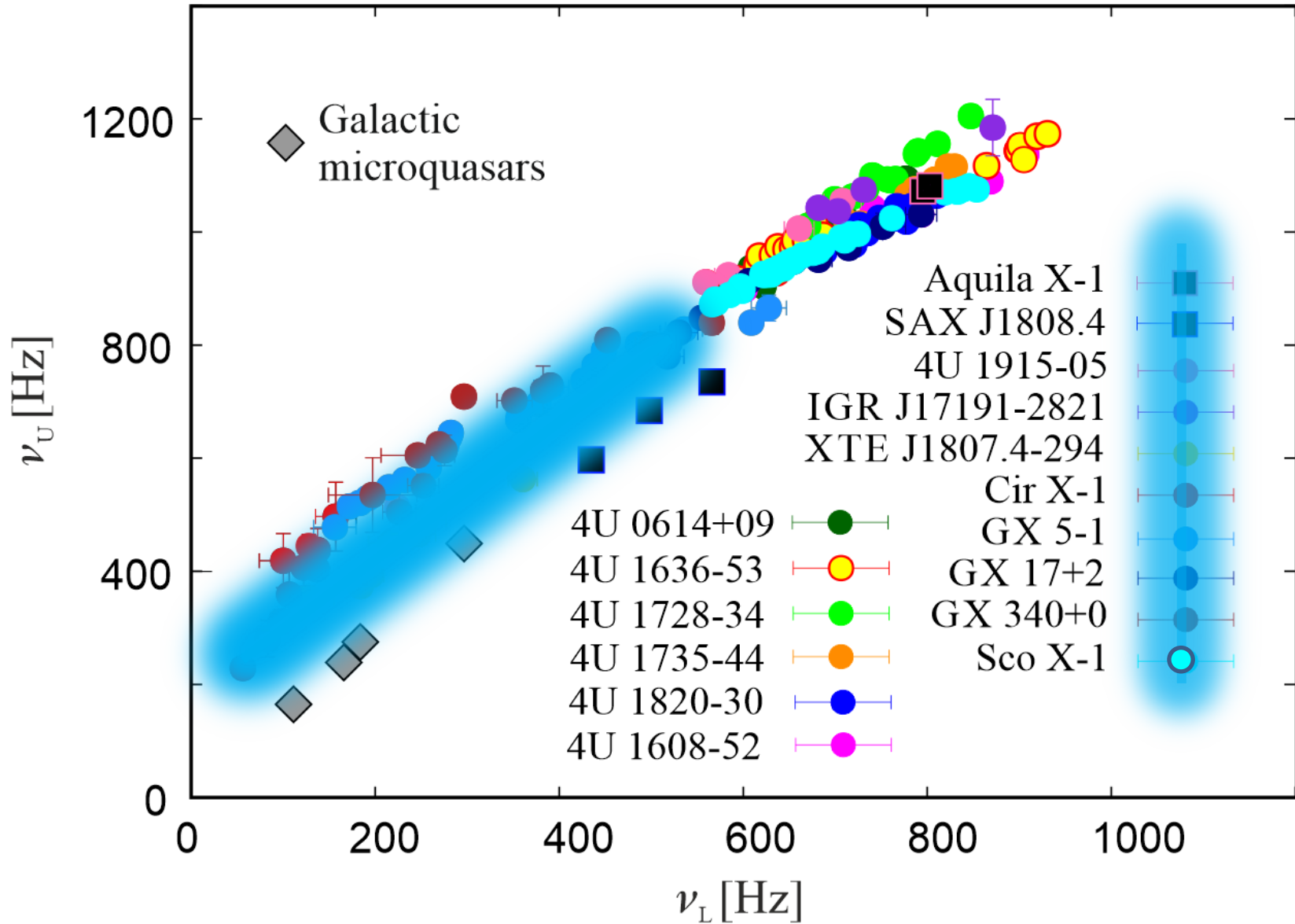
6. Conclusions (mass of atoll sources)



The consideration of fluid precession (CT model) provides better fits of the data of each source than the consideration of geodesic precession (RP model). The model predicts a lower NS mass than the RP model.

Source	Mass [M_{\odot}]	Source	Mass [M_{\odot}]	Source	Mass [M_{\odot}]
4U 0614+09	1.78	4U 1608-52	1.9	4U 1636-53	1.75
4U 1728-34	1.63	4U 1735-44	1.78	4U 1820-30	1.9

6. Conclusions (Z-sources, millisecond pulsars...)



7. Conclusions (Neutron Stars and Black Holes)

- The consideration of fluid precession (CT model) provides better fits of the NS data than the consideration of geodesic precession (RP model). The model predicts a lower NS mass than the RP model. *For the both simplified models, there is the same given fixed number of free parameters (degrees of freedom).*
(Torok et al. 2022, Apj; Klimovicova et al., in prep.).
- The consideration of fluid precession (CT model) leads to higher values of the estimated BH spin.
(Kotrlova et al. 2020, A&A, Torok et al. 2022, in prep.).

Thank you
for your attention

